2nd URSI AT-RASC, Gran Canaria, 28 May – 1 June 2018

Cyclostationary Source Separation in the Near-Field of Electronic Devices

Yury Kuznetsov[(1)], Andrey Baev[(1)], Michael Haider[(2)], Anastasia Gorbunova[(1)],
Maxim Konovalyuk[(1)], and Johannes A. Russer[(2)]
(1) Theoretical Radio Engineering Department, Moscow Aviation Institute, Russia
(2) Institute for Nanoelectronics, Technical University of Munich, Germany

1 Introduction

The electromagnetic field (EMF) emitted unintentionally by the printed circuit board (PCB) of an electronic device may cause interference to other devices in the vicinity of the PCB and thus, degrade their performance. The radiated EMF is stochastic in nature and usually contains cyclostationary components due to the data transferred between separate blocks along the surface of the PCB [1, 2]. Cyclostationarity of the emitted EMF may occur due to some regular processes intrinsic to the operating mode of the electronic device. For example, the electronic device could be programmed for sending several digital sequences carrying some coded information from the central processor unit (CPU) to some digital blocks (memory, connectors, and so on) on the surface of the PCB. These data sequences, when being sent over the strip lines of the multilayer PSB, usually have different physical parameters such as the duration of the single bit or bit rate, for reducing the interference due to the coupling between strip lines of the PCB.

Scanning of the EMF along a plane over the PCB in the near-field region by two ultra-wideband magnetic probes and subsequent synchronized recording of the measured signals by a real-time digital oscilloscope allows for extracting the correlation characteristics of the stochastic process for all scanned points [1, 3]. For registration of the radiated emissions, an automated two-point scanning system equipped with magnetic field probes can be used. Both probes must be connected via preamplifiers with similar frequency bandwidth to the corresponding inputs of the real-time digital oscilloscope which provides sufficient sampling rate. The measured signals need to be sampled synchronously over two parallel inputs of the oscilloscope. The measured data comprise the information about the unintentional radiation from the PCB, which can be extract by digital signal processing of the registered signals.

Due to the random nature of the data sequences and the superposition of the emitted fields produced by the surface currents flowing over the strip lines, the conventional averaging assuming wide sense stationary (WSS) properties of the stochastic process could not allow the separate identification of the parameters for simultaneously occurring radiations from several data sequences. Assuming the cyclostationary nature of the emitted fields can be useful for the separation of the whole process into deterministic, WSS and cyclostationary parts [3, 4]. Further processing of the cyclostationary part of the random process allows to separate the sources of the emitted fields and also to predict the spatial-time distribution of the correlation characteristics over the surface of the PCB for each identified source separately.

The theory of near-field scanning measurements over the equivalent Huygens surface in parallel to the object plane of the PCB is outlined in the next section. It shows the relation between the induced surface currents along the transmission lines of the PCB and the tangential components of magnetic field sensed by the near-field magnetic probe and the appropriate choice of the square meshes defined in both planes for appropriately capturing the information contained in the unintentional radiated emissions from the PCB of the electronic device [5].

Furthermore, a brief presentation of the theoretical background for the properties and characterization of the cyclostationary characteristics used for the cyclostationary source separation will be given. It is useful to keep in mind that the stochastic process is called cyclostationary if it reveals the periodicity of its statistical characteristics obtained by synchronized ensemble averaging of the proper functional obtained from the measured realization of the stochastic process. Another definition of the cyclostationary process exhibiting cyclo-ergodicity property assumes the existing of the nonzero complex exponential harmonic after averaging of the nonlinear inertia-less shifted transformation of the realization multiplied by the complex exponential harmonic [3, 4].

The measurement setup of the experimental investigation realizing the cyclostationary source separation will be presented in the final section of the paper. For the verification of the proposed algorithm the near-field scanning and subsequent time-domain registration of the measured signals were implemented using a scan system and real time digital oscilloscope [5]. The multifunctional electronic device under investigation was programmed for sending two different random bit sequences into predefined points on the surface of the PCB. The task was to separate these two random signals with different cyclostationary properties from the superposition of the fields emitted by different sources

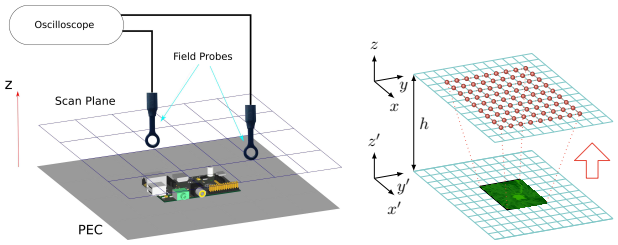

Figure 1. Device under test (DUT) with two field probes, connected to a multi–channel digital oscilloscope, in the scanning plane (left) and propagation of field-correlations to a further observation plane (right).

of the device under test and to define the space-time distributions of the separated sources over the equivalent Huygens surface.

2 Electromagnetic Field Modeling

Stationary stochastic electric and magnetic fields can be described by the dyadics

$$\underline{\underline{\Gamma}}_{H}(x_a,x_b,\tau) = \langle\!\langle H(x_a,t)H^{\dagger}(x_b,t-\tau)\rangle\!\rangle\,, \tag{1a}$$

$$\underline{\underline{\Gamma}}_{Pe}(x_a,x_b,\tau) = \langle\!\langle P_e(x_a,t)P_e^{\dagger}(x_b,t-\tau)\rangle\!\rangle\,, \tag{1b}$$

where $H(x,t)$ and Γ_{Pe} are the the time–windowed magnetic field and electrical source polarizations vectors, and the symbol † denotes the Hermitian conjugate. For $x_1 = x_2$ this function is the *autocorrelation function* of the field and for $x_1 \neq x_2$ it is the cross correlation function relating the field amplitudes at the points x_1 and x_2 [5–7]. With a Green's dyadic $G_{HPe}(x,t)$, relating the excited magnetic field $H(x,t)$ to the source electric polarization density, evolution of the magnetic field correlations can be obtained as [8]

$$\underline{\underline{\Gamma}}_{H}(x_a,x_b,\tau) = \iint_{V}\iint_{\tau',\tau''} G_{HPe}(x_a-x_a',\tau'') \times \underline{\underline{\Gamma}}_{Pe}(x_a',x_b',\tau-\tau')G_{HPe}^{\dagger}(x_b-x_b',\tau'-\tau'')d^3x_a'd^3x_b'd\tau'd\tau''. \tag{2}$$

Determining field correlations by means of a two-probe measurement system along a virtual mesh of sampling points and computation of the evolved field correlations is illustrated in Fig. 1.

3 Cyclostationary Characterization of the Stochastic Process

The model of any stochastic physical process $X(t)$ can be defined as a set of all possible time domain realizations of this process $x_i(t)\,; i \in \mathbb{Z}$, where $\mathbb{Z}$ is a set of all positive natural numbers. The cyclostationary process reveals the periodicity of its statistical characteristics obtained by appropriate averaging. The averaging assumes the knowledge of the period value T or equivalently the cyclic frequency $\alpha = 1/T$. The periodic sample mean function of the cyclostationary process $X(t)$ can be obtained from the realization $x(t)$ as [9]

$$m_X(\alpha,t) = \lim_{N\to\infty}\frac{1}{2N+1}\sum_{n=-N}^{N} x(t+nT) = \sum_{k=-\infty}^{\infty} \mathrm{e}^{\frac{\mathrm{j}2\pi kt}{T}} \lim_{\Delta\to\infty}\frac{1}{\Delta}\int_{-\frac{\Delta}{2}}^{\frac{\Delta}{2}} x(\xi)\,\mathrm{e}^{-\mathrm{j}2\pi\alpha k\xi}\,\mathrm{d}\xi\,. \tag{3}$$

The periodic second order moment function of the cyclostationary process $X(t)$ can be obtained by averaging the two-dimensional nonlinear inertialess shifted transformation $z(t,\tau)$ of the realization $x(t)$:

$$z(t,\tau) = x\left(t-\frac{\tau}{2}\right)x\left(t+\frac{\tau}{2}\right). \tag{4}$$

This transformation (4) can be used for evaluating the cyclic autocorrelation function, which is equivalent to the second order cyclic moment function [9]

$$R_x(\alpha,\tau) = \lim_{\Delta\to\infty}\frac{1}{\Delta}\int_{-\frac{\Delta}{2}}^{\frac{\Delta}{2}} z(t,\tau)\,\mathrm{e}^{-\mathrm{j}2\pi\alpha t}\,\mathrm{d}t\,. \tag{5}$$

The subtraction of the periodic sample mean function (3) from the realization of the stochastic process $x(t)$ with subsequent two-dimensional nonlinear inertialess shifted transformation gives the non-periodic second order cyclic cumulant function:

$$C_X(\alpha,\tau) = \lim_{\Delta\to\infty}\frac{1}{\Delta}\int_{-\frac{\Delta}{2}}^{\frac{\Delta}{2}} \left[x\left(t-\frac{\tau}{2}\right) - m_X\left(\alpha,\left(t-\frac{\tau}{2}\right)\right)\right] \times \left[x\left(t+\frac{\tau}{2}\right) - m_X\left(\alpha,\left(t+\frac{\tau}{2}\right)\right)\right]\mathrm{e}^{-\mathrm{j}2\pi\alpha t}\,\mathrm{d}t\,. \tag{6}$$

The separation procedure for cyclostationary stochastic signals with different cyclic frequencies $\alpha_1 = 1/T_1$ and $\alpha_2 = 1/T_2$ can be implemented by using the cyclic cross-correlation cumulant function (CCCF) between the reference cyclostationary process $Y(t)$ defined in some point over the PCB and synchronously registered stochastic process in one of the scanned points in the equivalent Huygens surface in parallel to the object plane of the PCB $X_{mn}(t)$, where m is the number of the column and n is the number of the row in the rectangular mesh of the scanning plane. For example, the cyclic CCCF for cyclic frequency α_1 is defined as follow:

$$C_{YX_{mn}}(\alpha_1,\tau) = \lim_{\Delta\to\infty}\frac{1}{\Delta}\int_{-\frac{\Delta}{2}}^{\frac{\Delta}{2}} \left[y\left(t-\frac{\tau}{2}\right) - m_y\left(\alpha_1,\left(t-\frac{\tau}{2}\right)\right)\right] \times \left[x_{mn}\left(t+\frac{\tau}{2}\right) - m_{x_{mn}}\left(\alpha_1,\left(t+\frac{\tau}{2}\right)\right)\right]\mathrm{e}^{-\mathrm{j}2\pi\alpha_1 t}\,\mathrm{d}t\,. \tag{7}$$

The physical meaning of the cyclic CCCF (7) is the space-time shift dependence of the amplitude and initial phase for

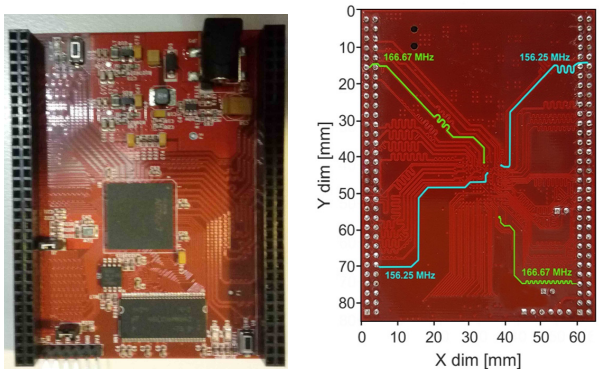

(a) (b)

Figure 2. Development board with FPGA as device under test (DUT), top (a) and bottom (b) view.

the complex harmonic with cyclic frequency α_1, while the amplitude of this harmonic reveals the correlation between the reference cyclostationary process and the cyclostationary process in the $\{m,n\}$ point of the mesh with the same cyclic frequency α_1.

4 Experimental Measurement Results

The measurement setup is shown schematically in Fig. 1. For measuring the radiated emission, an in-house two-probe scanning system equipped with Langer EMV-Technik RF-R 50-1 magnetic field probes with a frequency bandwidth from 30 MHz to 3 GHz. Both probes were connected through the Langer PA 303 preamplifiers with a frequency band from 100 kHz to 3 GHz to the corresponding inputs of the 13 GHz Serial Data Analyzer LeCroy SDA 813Zi-A. The sampling rate of the digitizer is up to $F_s = 40\,\mathrm{GS\,s^{-1}}$. The measured signals were sampled synchronously over two parallel inputs of the oscilloscope.

For verification of the proposed cyclostationary source separation algorithm, a multifunctional digital electronic device was chosen. The photo of this device, a multilayered PCB development board with a Xilinx FPGA Artix 7, is shown Fig. 2. The FPGA of the device was programmed for sending two random bit sequences with different bit rates to some predefined outputs on the surface of the PCB. The output points and the traces of differential strip lines chose for random bit sequences transferring from FPGA to the corresponding outputs are shown schematically on the photo of the PCB surface (see Fig. 2 (b)). The bit rates for two random sequences were defined as $\alpha_1 = \frac{1}{T_1} = \frac{1}{6}\mathrm{GHz} = 166.67\,\mathrm{MHz}$ and $\alpha_2 = \frac{1}{T_2} = \frac{1}{6}\mathrm{GHz} = 156.25\,\mathrm{MHz}$. For the near-field scanning, scanning points were defined on a rectangular mesh with 5 mm spacing between adjacent points. The total number of scanning points is (18×16). The reference probe was situated on the other side of the PCB near the point where neighboring signal lines carry outputs of both sequences.

The sampling frequency of the real time digital oscilloscope was defined as $10\,\mathrm{GS\,s^{-1}}$, and the number of samples registered during each run for all scanning points was choosen as 5 million. After implementing the averaging algorithms in accordance to (7), the cyclic CCCFs were obtained $C_{YX_{mn}}(\alpha_1,\tau)$ and $C_{YX_{mn}}(\alpha_2,\tau)$ for each sampling point in the scanning plane. The amplitude values of cyclic CCCFs in logarithmic color scale for some defined time shift τ presented in Fig. 3, show the spatial distributions of the evaluated cyclic statistical characteristics, each of which resembles the geometric configuration of the transmission strip lines shown in Fig. 2 (b).

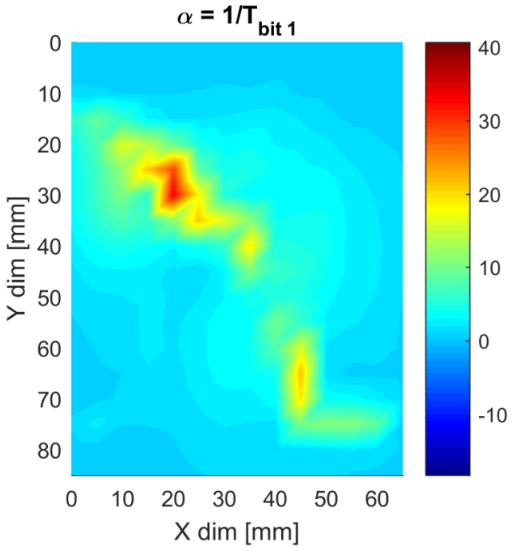

(a) $\alpha_1 = 1/T_1$

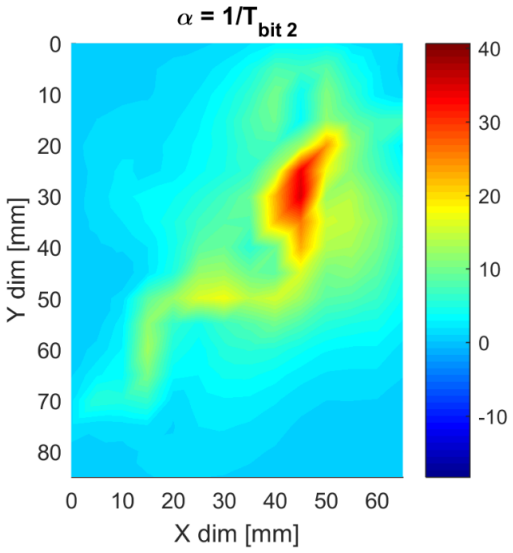

(b) $\alpha_2 = 1/T_2$

Figure 3. Spatial distributions of two cyclic cross-correlation cumulant functions.

Thus, the results of the described experiment confirm the capability of the proposed algorithm tp perform cyclostationary source separation in the near-field of the electronic device under test.

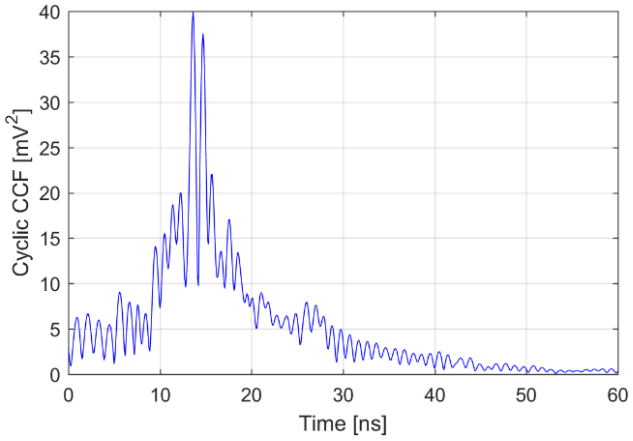

(a) $\alpha_1 = 1/T_1$

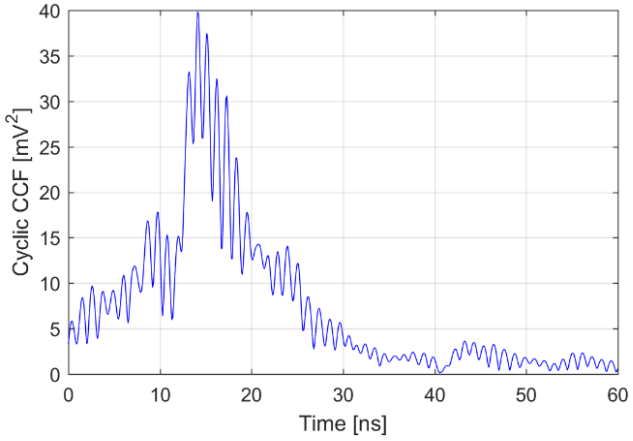

(b) $\alpha_2 = 1/T_2$

Figure 4. Cyclic cross-correlation cumulant functions.

The comparison of two CCCFs $C_{YX_{mn}}(\alpha_1, \tau)$ and $C_{YX_{mn}}(\alpha_2, \tau)$ can be carried out by using their representation in Fig. 4. It can be seen that both CCCFs have the global maximum for some specified time shift between the reference and sampled stochastic processes, which can be explained by a delay between registered realization due to the final speed of signal propagation and possibly the different lengths of connecting cables. The shape of each cyclic CCCF is defined by the shape and duration of the measured bit signal, which are slightly different for used random sequences. The fluctuation of both cyclic CCCFs can understood by some parasitic residue deterministic signal received by magnetic probes during the experiment.

5 Conclusion

Near-field scanning of the stochastic electromagnetic field radiated by a multifunctional electronic device has been performed and field correlations have been analyzed. Cyclostationarity of the emitted field has been investigated and an algorithm has been demonstrated to perform source separation in the near-field of the device under test. Cyclic cross-correlation cumulant functions for the electromagnetic near-field have been determined.

6 Acknowledgments

This work was supported by the European Union's Horizon 2020 research and innovation programme under grant no. 664828 (NEMF21) and by the COST action IC1407.

References

[1] Y. Kuznetsov, A. Baev, A. Gorbunova, M. Konovalyuk, J. A. Russer, M. Haider, and P. Russer, "Cross-correlation analysis of the cyclostationary near-field unintentional radiations from the PCB," in *Proc. Int. Symp. on Electromagn. Compat., EMC*, Angers, France, Sep 4-8 2017.

[2] J. A. Russer, P. Russer, M. Konovalyuk, A. Gorbunova, A. Baev, and Y. Kuznetsov, "Near-field propagation of cyclostationary stochastic electromagnetic fields," in *Int. Conf. on Electromagn. in Advanced Applications (ICEAA), 2015*, Torino, Italy, Sep 2015, pp. 1456–1459.

[3] P. P. J. Schreier and P. L. L. Scharf, *Statistical Signal Processing of Complex-Valued Data: The Theory of Improper and Noncircular Signals*, 1st ed. Cambridge, New York: Cambridge University Press, 2010.

[4] W. A. Gardner, A. Napolitano, and L. Paura, "Cyclostationarity: Half a century of research," *Signal Processing*, vol. 86, no. 4, pp. 639–697, Apr. 2006.

[5] J. A. Russer and P. Russer, "Modeling of noisy EM field propagation using correlation information," *IEEE Trans. Microw. Theory Techn.*, vol. 63, no. 1, pp. 76–89, Jan 2015.

[6] W. B. Davenport and W. L. Root, *An Introduction to the Theory of Random Signals and Noise*. New York: McGraw-Hill, 1958.

[7] J. A. Russer and P. Russer, "An efficient method for computer aided analysis of noisy electromagnetic fields," in *IEEE MTT-S International Microwave Symposium Digest*, Jun. 2011, pp. 1–4.

[8] J. A. Russer and M. Haider, "Time-domain modeling of noisy electromagnetic field propagation," in *Proceedings of the IEEE International Microwave Symposium*, Philadelphia, PA, Jun. 10-15 2018.

[9] W. A. Gardner, "The spectral correlation theory of cyclostationary time-series," *Signal Processing*, vol. 11, no. 1, pp. 13 – 36, 1986.